nzsee
NEW ZEALAND SOCIETY FOR EARTHQUAKE ENGINEERING

Wall-to-floor connection behavior in a low-damage concrete wall building

Q. Yang, R.S. Henry & Y.Q. Lu
University of Auckland, Auckland.

ABSTRACT

Following the 2010/2011 Canterbury earthquakes, approximately 60% of multi-story buildings with reinforced concrete walls required demolition. Both practitioners and researchers have increasingly realized that low-damage structural systems could be an alternative to improve the seismic behavior of concrete buildings and to reduce the economic and social impact of structural damage in future earthquakes. To verify the seismic response of a low-damage concrete wall building representing state-of-art design practice, a shake table test on a two-story concrete building was recently conducted as part of an ILEE-QuakeCoRE collaborative research program. The building utilized flexible wall-to-floor connections in the long span direction and isolating wall-to-floor devices in the short span direction to provide a comparison of their respective behavior. Additionally, the wall-to-floor interaction such as effects of wall uplift on the link slab, quantification of gap in the tongue connection, and acceleration transfer mechanism from floor to the wall will be discussed in this paper.

1 INTRODUCTION

Following the 2010/2011 Canterbury earthquakes, approximately 60% of multi-story buildings with reinforced concrete walls required demolition [1]. The increasing need to reduce post-earthquake damage and downtime to modern buildings has led to the development of the low-damage design philosophy where earthquake demands can be resisted with damage confined to easily replaceable components. Since the late 1990's, a large number of different unbonded PT wall systems have been investigated by researchers [2-8], which has led to the publication of design methods and guidelines. Buildings incorporating low-damage structural systems have also been constructed in New Zealand, including the Southern-Cross hospital building in Christchurch that withstood the Canterbury earthquakes [9]. With unbonded PT component design and performance well established, researchers have shifted focus to interaction between structural components in buildings. The behavior of alternative wall-to-floor connections in PT wall buildings was investigated using numerical models [10] and innovative connectors have been tested that can isolate the floor from the vertical uplift of the wall while still maintaining a horizontal load path [11]. In addition, large-scale subassembly tests confirmed that significant deformations and damage are induced in floors when connected integrally with a PT wall and showed that the use of an isolated wall-to-floor connection could

successfully reduce out-of-plane floor deformations to ensure a more predictable lateral-load response [12]. To verify the seismic response of a low-damage concrete wall building representing state-of-art design practice, a shake table test on a two-story concrete building was recently conducted as part of an ILEE-QuakeCoRE collaborative research program. The building utilized flexible wall-to-floor connections in the long span direction and isolating wall-to-floor devices in the short span direction to provide a comparison of their respective behavior. Additionally, the wall-to-floor interaction such as effects of wall uplift on the link slab, quantification of gap in the tongue connection, and acceleration transfer mechanism from floor to the wall will be discussed in this paper.

2 EXPERIMENTAL PROGRAM

2.1 Detailing of wall-to-floor connections

Two alternative wall-to-floor connection designs were implemented to accommodate the potential displacement incompatibility as the wall uplifts, with drawings shown in Figure 1. A flexible wall-to-floor connection was used for the Grid 1 and 3 walls in the longitudinal direction that were designed to be stiff enough to transfer in-plane diaphragm loads while being flexible in the out-of-plane direction to accommodate wall uplift and rotation. On Level 2, the composite floor provided sufficient flexibility when spanning perpendicular to the wall, and on Level 1 a 600 mm wide and 80 mm thick link slab was located between the wall and the first double tee unit. Isolated wall-to-floor connections were used for the Grid A and C walls in the transverse direction with the configuration of the frames such that the wall was not required to resist gravity loads for the floors. A steel tongue that was embedded in the beam extended out into an armored slot that was cast in the wall panels. An initial 10 mm gap was designed into the steel tongue connection for tolerance that was later filled with high density plastic shims. Pinned struts were used to provide an out-of-plane connection at the ends of the wall on both floor levels.

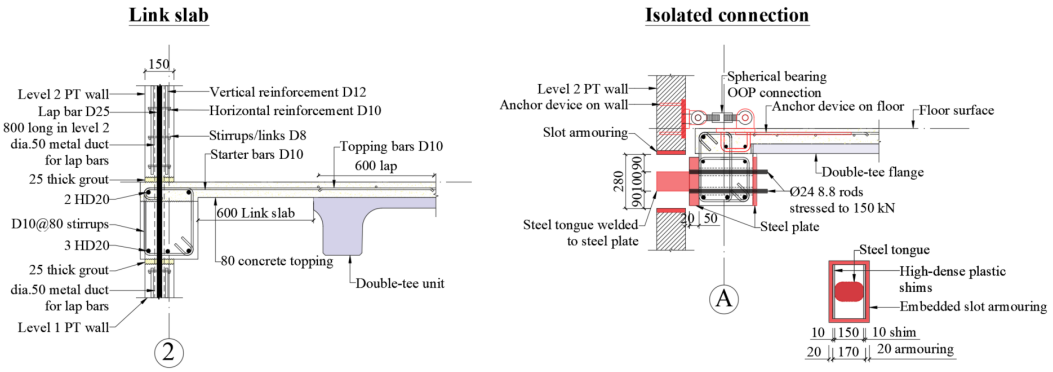

Figure 1: Detailing of wall-to-floor connections

2.2 Instrumentation

The test building was instrumented with a dense array of sensors consisting of a total of 360 channels of data recorded at 256 Hz to monitor the overall building response as well as local component responses. As illustrated in Figure 2, for wall-to-floor connections, triaxial accelerometers were placed in four locations on each floor slab, and on one wall in each direction at the floor levels. Out-of-plane floor deflections at 16 locations were measured by string-pot displacement gauges extending vertically from the shake-table to the bottom of the level 1 floor and from top of the level 1 floor to the bottom of level 2 floor.

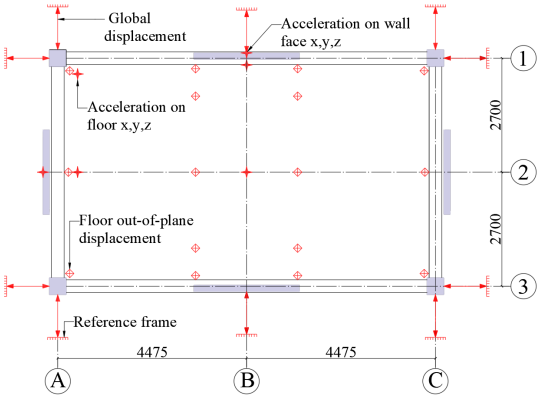

Figure 2: Instrumentation for wall-to-floor connections

2.3 Ground motions and test sequence

Ground motions were selected to represent the seismic hazard for soil class C in Wellington, New Zealand, including serviceability limit state (SLS) at 25% and 50% of design level intensity, ultimate limit state (ULS) at 100% design level intensity, and maximum consider earthquake (MCE) at 180% design level intensity. Ground motions were selected from existing datasets [13, 14] that were generally spectrum compatible over the building period range and that has similar intensity for both components. Test labels follow a format of 'Design'-'Intensity'-'GM'-'Direction'.

3 DISCUSSIONS

3.1 Damage state

The mapped crack patterns on the top of both floors at the conclusion of testing are illustrated in Figure 3. For the Level 1 floor the cracking was almost entirely contained within the flexible link slabs. The distributed cracking in the link slab occurred as it accommodated the vertical deformations of the wall and connected beams while the double tees remained stiff and undamaged. On the Level 2 floor the cracking was concentrated in the region adjacent to Walls 1 and 3 and extended into the center of the floor. The residual crack widths at the conclusions of each series of tests are summarized in Table 1.

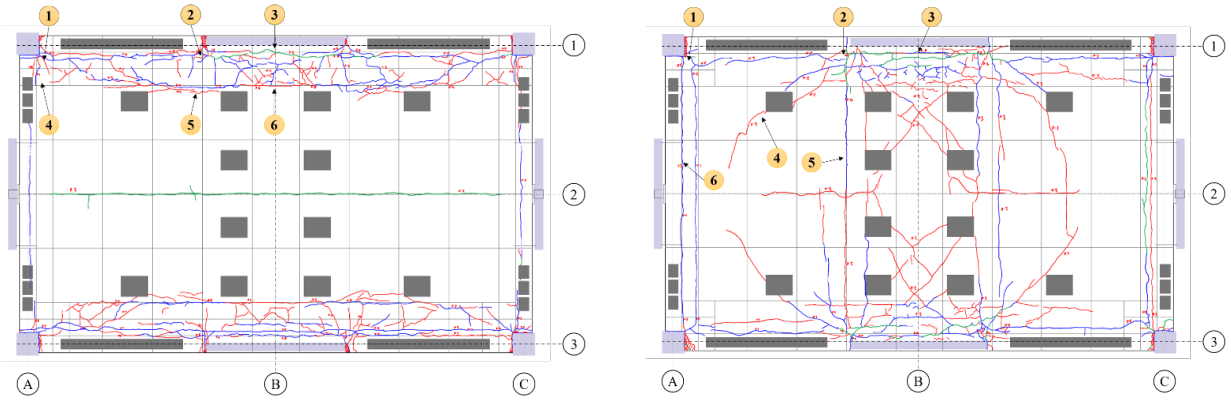

(a) Level 1 *(a) Level 2*

Figure 3: Floor crack pattern at end of testing

Table 1: Residual crack widths on the floor.

	D1a-25%	D1a-100%	D2-100%	D2-180%	D3-150%
Max	0.2 mm	0.4 mm	0.5 mm	1.0 mm	1.2 mm
Typical	<0.1 mm	<0.2 mm	0.2 mm	0.2 mm	0.2 mm

3.2 Wall uplift accommodated by link slab

For flexible wall-to-floor connections, a ratio of deformation of link slab to wall uplifts was calculated to quantify the effect of wall uplifting on the damage to the floors. Figure 4 illustrates the floor profiles of Levels 1 and 2 in the transverse direction when one end of Grid 1 wall maximally uplifted. The ratio can be calculated as follows.

$$r_i = \frac{d_1^{(i)} - d_{1i}^{(i)}}{d_1^{(i)} - d_2^{(i)}} \; i = 1, 2 \tag{1}$$

where i represents for the level; $d_1^{(i)} - d_2^{(i)}$ represents for the overall uplift excluding floor vibration at the center and possible wire stretching; $d_1^{(i)} - d_{1i}^{(i)}$ represents for the wall uplift accommodated by the link slab. It should be here that $d_1^{(i)} - d_{1i}^{(i)}$ represents for wall uplift accommodated by the slab within the range of line 1 to line 1i for Level 2.

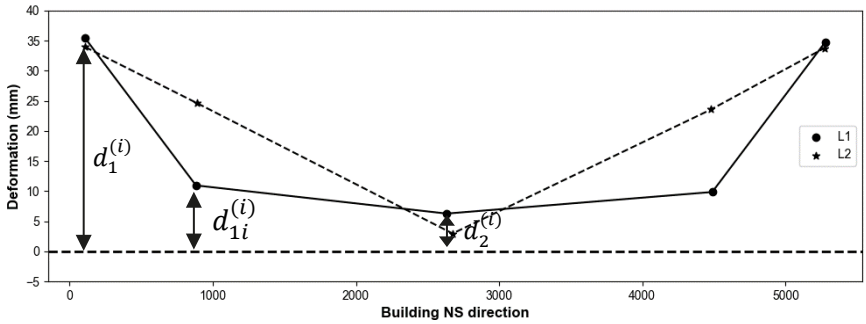

Figure 4: Floor profiles in the transverse direction

The trend of r_i throughout x-directional tests from D1a-100%-FF-x is illustrated in Figure 5. It is observed that the link slab on Level 1 averagely accommodated 85% of wall uplift while Level 2 averagely accommodated 35 % of wall uplift, which confirmed that cracks extend to the floor center on Level 2 while cracks almost concentrated within the link slab on Level 1.

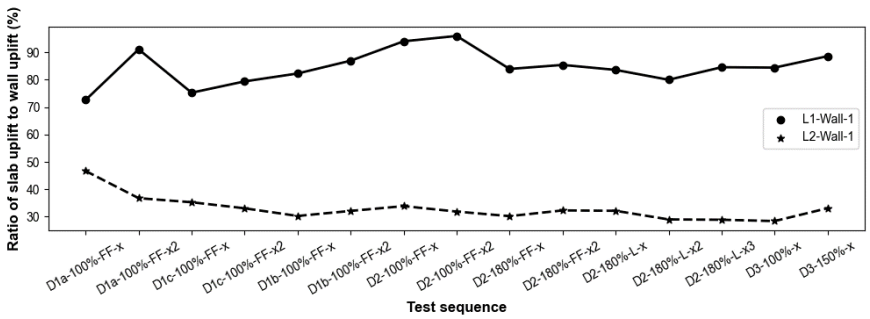

Figure 5: The trend of r_i throughout x-directional tests

3.3 Quantification of tongue gap

For isolated wall-to-floor connections, the gap into the steel tongue connection was a critical factor that affected the dynamic characteristics of the building. Therefore, the quantification of the gap was necessary for investigating its effects on the dynamic characteristics such as period in the NS direction. Figure 6 illustrates the relative horizontal deformations measured between the wall and the steel tongue of the isolated connection for D2-180%-FF-y. The actual gap can be defined as the distance between the upper bound and lower bound of the measured horizontal displacement profile. The process of determining the actual gap followed three main steps: (1) filter the raw data to eliminate the high frequency noises such as wire vibrating due to the tongue impact; (2) set up a window to extract peak points from the time domain during which the tongue engaging with the side of the slot; (3) fit these peak points to find the upper bound and lower bound. The actual gap into Tongue A on Levels 1 and 2 is illustrated in Figure 7. The actual gap fluctuated throughout the test series. As test series progress, shims became squashed and bent, resulting in an increase in the gap. In contrast, the gap reduced when shims were replaced.

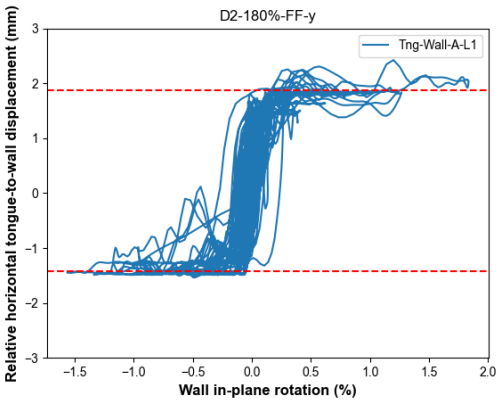

Figure 6: Isolated wall-to-floor connection response (Wall A Level 1) for test D2-180%-FF-y

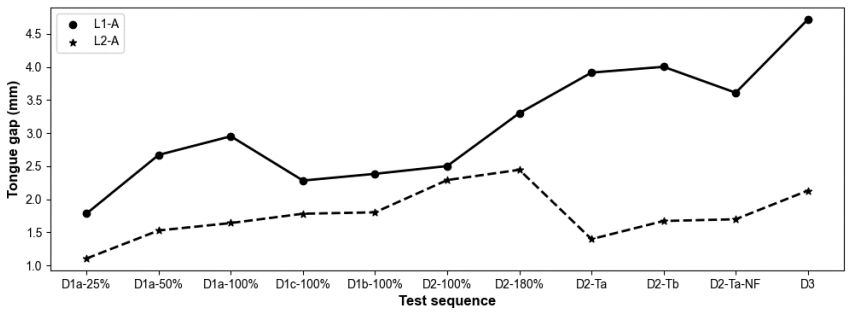

Figure 7: The actual tongue gap throughout test series

Figure 8 illustrates the relationship between the tongue gap and the period of building in the NS direction. The dispersion of data in the plot showed a pattern that the gap increases with the increasement of the period, and the location of the tongue connection is a key feature that affect the gap. Considering that the lack of design recommendations for determining the gap in the tongue connection, a formula for designing the gap in term of the period is necessary. For simplicity, a linear model was proposed based on the following principles: (1) the line separates the data into different regions, as each independent region represents for the tongue connection on different levels; (2) optimize the summation of distance from all points in the plot to the line to minimum. Therefore, the red line calculated based on support vector machine was calculated.

Notably, this formula was obtained according to statistics, therefore, more data can contribute to its effectiveness. On the other hand, only period of the building was considered in the formula, and other dynamic characteristics such as the frequency of wall rocking can be accounted for to improve the formula.

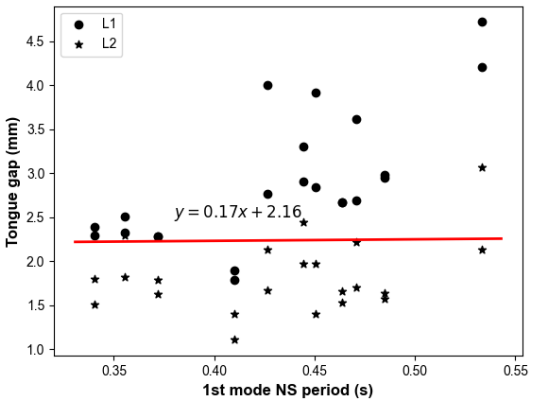

Figure 8: Relationship between the tongue gap and the period of building in the NS direction

3.4 Acceleration transfer from wall to floor

The building utilized two types of wall-to-floor connection as alternatives to low-damage. To theoretically analyze the acceleration transfer mechanism from wall to floor and compare their performance, signal processing using acceleration time-series data including Fast Fourier Transformation (FFT), and correlation analysis was implemented.

3.4.1 Similarity

The change of acceleration time-series data from wall to floor implied the acceleration transfer mechanism for the connections. However, the features that can discriminate two signals need to perform FFT to allow data transfer from the time domain to the frequency domain. In the frequency domain, the original signal was converted to a distribution of which random variable is the frequency and probability is the amplitude. Therefore, the similarity of the distributions from wall to floor using FFT can quantify the acceleration transfer. High KL divergence means that the two distributions have low similarity. To measure the similarity, the KL divergence of two distributions $p(f)$ and $q(f)$, denoted $D_{KL}(p(f)||q(f))$ can be calculated, as shown in Eq. (2).

$$D_{KL}(p(f)||q(f)) = \sum_{f\epsilon\mathcal{F}} p(f) ln \frac{p(f)}{q(f)} \quad (2)$$

where $\mathcal{F}$ is the set of the frequency.

Figure 9 illustrates the Fourier spectra of acceleration time-series data from wall to floor for flexible and isolated connections. The KL divergence of acceleration transfer for isolated connections was significantly higher than that for flexible connections, which confirmed that the isolated connection switched the acceleration transfer mechanism while the flexible connection can fully transfer the acceleration. For isolated connection, the difference in the horizontal transfer mainly attributed to the high frequency components due to the tongue impact. In contrast, the difference in the vertical transfer was concentrated in the domain of low frequency due to the wall rocking.

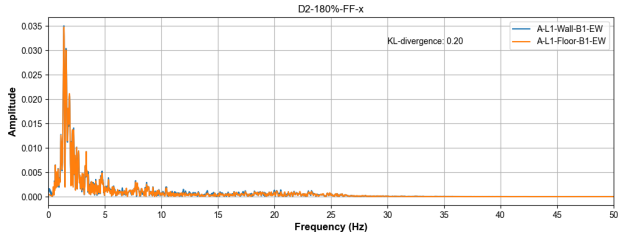

(a) Horizontal transfer for flexible connection

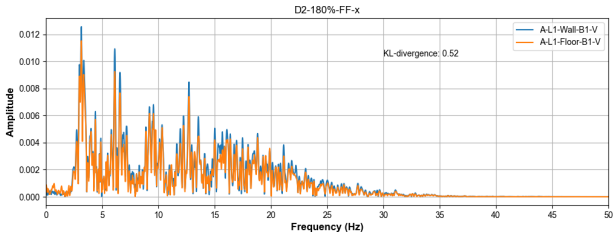

(b) Vertical transfer for flexible connection

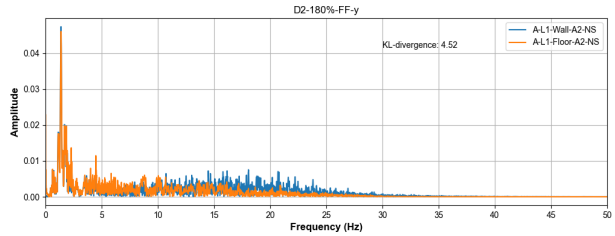

(c) Horizontal transfer for isolated connection

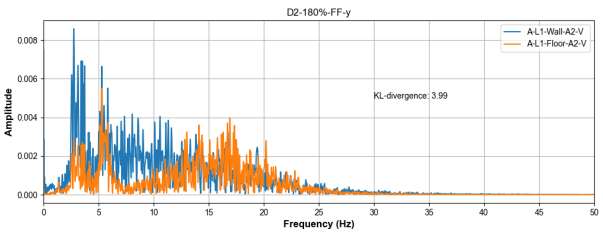

(d) Vertical transfer for isolated connection

Figure 9: Acceleration transfer for D2-180 tests

Tables 2 and 3 summarize the KL divergence of horizontal and vertical transfer for flexible connections and isolated connections, respectively. For flexible connections, the similarity of horizontal and vertical transfer on Level 1 is higher than that on Level 2. This is because the rigidity of link slab was lower than that of composite floor, resulting in its better performance in transferring accelerations.

Table 2: KL divergence of horizontal and vertical transfer for the flexible connections.

	D1a-50%		**D1a-100%**		**D2-100%**		**D2-180%**		**D2-180%-L**	
Level	1	2	1	2	1	2	1	2	1	2
Horizontal	0.12	0.24	0.18	0.43	0.17	0.30	0.37	0.82	0.48	0.83
Vertical	0.14	0.94	0.19	0.73	0.25	1.26	0.62	2.65	0.64	3.98

Table 3: KL divergence of horizontal and vertical transfer for the isolated connections.

	D1a-50%		**D1a-100%**		**D2-100%**		**D2-180%**	
Level	1	2	1	2	1	2	1	2
Horizontal	1.65	7.32	1.89	7.10	2.54	9.31	4.52	15.99
Vertical	0.24	0.56	1.16	2.18	1.53	1.75	3.99	4.33

3.4.2 Coherence estimate

The KL divergence of acceleration transfer demonstrated the similarity of Fourier spectra from wall to floor, however, coherence estimate is necessary to further investigate the frequency domain in which acceleration signals between wall and floor are correlated. Coherence values tending towards 0 indicate that the

corresponding frequency components are uncorrelated while values tending towards 1 indicate that the corresponding frequency components are correlated. Figures 10 and 11 illustrate the coherence estimates for horizontal transfer and vertical transfer in D2-180 test, respectively. The red dots in the plots represent for the frequency at which the coherence value is larger than 0.95.

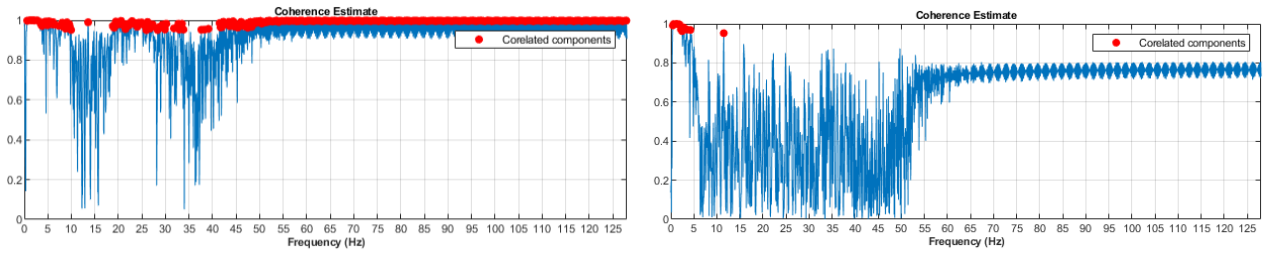

(a) Flexible connection *(b) Isolated connection*

Figure 10: Coherence estimate for horizontal transfer in D2-180 test

For flexible connection, horizontal acceleration almost fully transferred from wall to wall as the correlated components are thorough the entire frequency domain. For isolated connection, only frequency components within 5Hz are correlated, which shows that the tongue can transfer the horizontal acceleration by impacting.

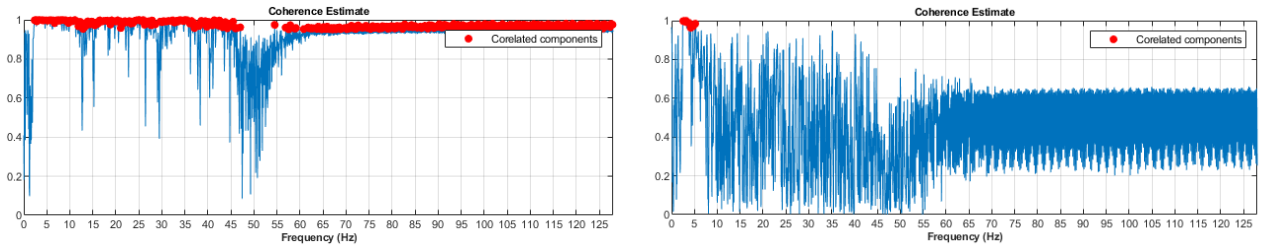

(a) Flexible connection *(b) Isolated connection*

Figure 11: Coherence estimate for vertical transfer in D2-180 test

For flexible connection, vertical acceleration almost fully transferred from wall to wall like horizontal accelerations. For isolated connection, only frequency components around 5Hz are correlated, which confirmed that wall the effect of wall rocking can transfer to the floor by the tongue sliding.

4 CONCLUSIONS

This paper presents analytical results of flexible and isolated wall-to-floor connections in a low-damage building. The following conclusions were drawn from the analyses:

1. 1. The link slab on Level 1 averagely accommodated 85% of wall uplift while Level 2 averagely accommodated 35 % of wall uplift, which confirmed that cracks extend to the floor center on Level 2 while cracks almost concentrated within the link slab on Level 1.
2. 2. The actual gap into the steel tongue was quantified based on the isolated wall-to-floor connection response. In addition, the model for determining the gap using the period was proposed.
3. 3. Acceleration transfer mechanism was studied with the assistant of FFT and coherence estimate. The results showed that flexible connection can fully transfer acceleration while isolated connection can effectively transfer acceleration by tongue impacting and sliding.

REFERENCES

[1] Marquis, F., Kim, J. J., Elwood, K. J., and Chang, S. E., Understanding post-earthquake decisions on multi-storey concrete buildings in Christchurch, New Zealand[J]. Bulletin of Earthquake Engineering, 2017. 15(2):731-758.

[2] Sritharan, S., S. Aaleti, R.S. Henry, K.Y. Liu, and K.C. Tsai, Precast concrete wall with end columns (PreWEC) for earthquake resistant design. Earthquake Engineering & Structural Dynamics, 2015. 44(12):2075-2092.

[3] Henry, R.S., Brooke, N.J., Sritharan, S., and Ingham, J.M., Defining concrete compressive strain in unbonded post-tensioned walls. ACI Structural Journal, 2012. 109(1): 101-112.

[4] Twigden, K.M., Dynamic Response of Unbonded Post-tensioned Concrete Walls forSeismic Resilient Structures, 2016, PhD Thesis, University of Auckland: Auckland, New Zealand.

[5] Perez, F.J., Pessiki, S., and Sause, R., Experimental lateral load response of unbonded post-tensioned precast concrete walls. ACI Structural Journal, 2013. 110(6): 1045-1055.

[6] Holden, T., Restrepo, J., and Mander, J.B., Seismic performance of precast reinforced and prestressed concrete walls. Journal of Structural Engineering, 2003. 129(3): 286-296.

[7] Marriott, D., Pampanin, S., Bull, D., and Palermo, A., Dynamic testing of precast, posttensioned rocking wall systems with alternative dissipating solutions. Bulletin of the New Zealand Society for Earthquake Engineering, 2008. 41(2): 90-103.

[8] Sahami, K., Veismoradi, S., Zarnani, P., and Quenneville, P., Seismic Performance of Rocking Concrete Shear Walls with Innovative Rotational Resilient Slip Friction Joints. Pacific Conference on Earthquake Engineering, 2019. Auckland, New Zealand.

[9] Pampanin, S., Kam, W.Y., Haverland, G., and Gardiner, S., Expectation meets reality: Seismic performance of posttensioned precast concrete Southern Cross Endoscopy building during the 22nd Feb 2011 Christchurch., 2011, New Zealand Concrete Industries Conference, Rotorua, New Zealand.

[10] Henry R S, Sritharan S, Ingham J M. Finite element analysis of the PreWEC self-centering concrete wall system. Engineering Structures, 2016; 115: 28-41.

[11] Watkins J, Sritharan S, Henry R S. An experimental investigation of a wall-to-floor connector for self-centering walls. in Proceedings of the Tenth U.S. National Conference on Earthquake Engineering. 2014. Anchorage, Alaska.

[12] Liu Q, French C W, Sritharan S. Performance of a Precast Wall with End Columns RockingWall System with Precast Surrounding Structure. ACI Structural Journal, 2020; 117(3): 103-116.

[13] Yeow T Z, Orumiyehei A, Sullivan T J, MacRae G A, Clifton G C, Elwood K J. Seismic performance of steel friction connections considering direct-repair costs. Bulletin of Earthquake Engineering, 2018; 16(12): 5963-5993.

[14] FEMA P-695. Federal Emergency Management Agency. Quantification of Building Seismic Performance Factors, FEMA. Washington DC, USA: 2009